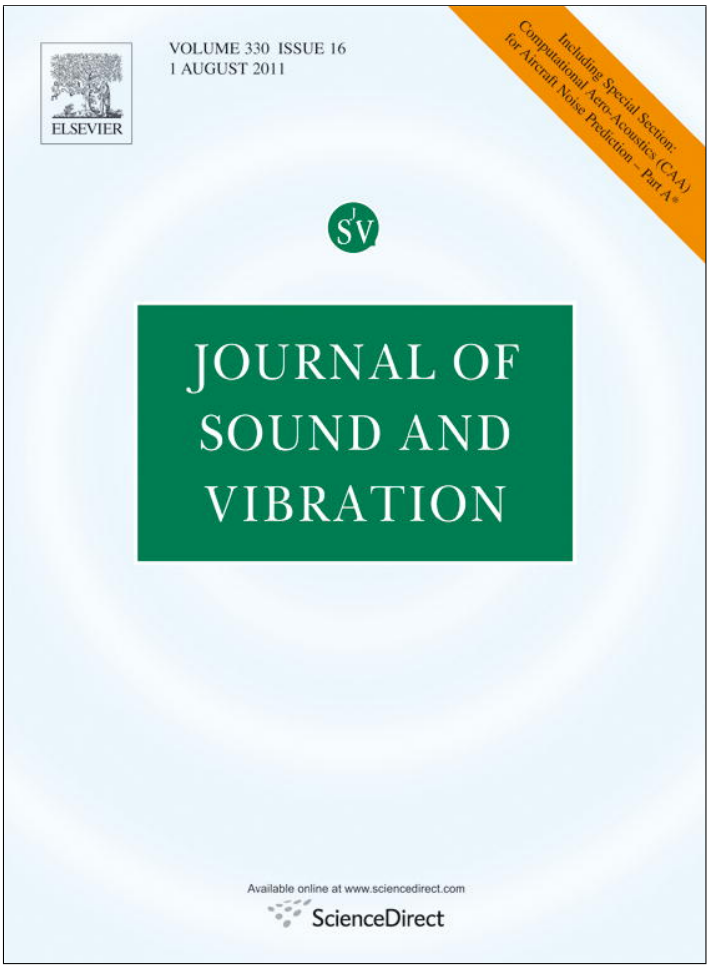

Journal of Sound and Vibration 330 (2011) 4029–4046

Contents lists available at ScienceDirect

Journal of Sound and Vibration

journal homepage: www.elsevier.com/locate/jsvi

Scattering by cavities of arbitrary shape in an infinite plate and associated vibration problems

Michael J.A. Smith [a,*], Michael H. Meylan [a], Ross C. McPhedran [b]

[a] Department of Mathematics, University of Auckland, Private Bag 92019, Auckland, New Zealand
[b] CUDOS ARC Centre of Excellence, School of Physics, University of Sydney, Sydney, New South Wales 2006, Australia

ARTICLE INFO

Article history:
Received 31 December 2010
Received in revised form
15 March 2011
Accepted 20 March 2011
Handling Editor: L.G. Tham
Available online 14 April 2011

ABSTRACT

This paper presents a solution for the displacement of a uniform elastic thin plate with an arbitrary cavity, modelled using the biharmonic plate equation. The problem is formulated as a system of boundary integral equations by factorizing the biharmonic equation, with the unknown boundary values expanded in terms of a Fourier series. At the edge of the cavity we consider free-edge, simply-supported and clamped boundary conditions. Methods to suppress ill-conditioning which occurs at certain frequencies are discussed, and the combined boundary integral equation method is implemented to control this problem. A connection is made between the problem of an infinite plate with an arbitrary cavity and the vibration problem of an arbitrarily shaped finite plate, using the jump discontinuity present in single-layer distributions at the boundary. The first few frequencies and modes of displacement are computed for circular and elliptic cavities, which provide a check on our numerics, and results for the displacement of an infinite plate are given for four specific cavity geometries and various boundary conditions.

1. Introduction

The problem of computing the vibration of thin elastic plates of finite size subject to various boundary conditions has been widely studied (Leissa [1], Graff [2], Itao and Crandall [3], Leissa and Narita [4]). These papers have been focused primarily on determining the modes of vibrations. By comparison the problem of wave scattering by infinite plates has received considerably less attention. This is in contrast to the case for membranes, where the problem of scattering for the Helmholtz equation is nearly as well-studied as the eigenvalue problem for the Laplacian. The simplest problem which can be considered for the infinite plate is wave scattering by a single circular cavity. This was considered by Konenkov [5], Norris and Vemula [6] and recently has been extended to an array of circular cavities by Movchan et al. [7], Parnell and Martin [8]. The problem of wave scattering by a cavity is strongly connected with crack problems in plate and shell theory, since a crack may be thought of as a degenerate cavity. However, it appears that only straight line cracks, and not cracks of arbitrary shape have been solved for (Andronov and Belinskii [9], Porter and Evans [10]).

If the geometry of the cavity is considered to be circular then the solution can be found by separation of variables, in terms of Bessel functions. Similarly, if the cavity is elliptical a solution can be found in terms of Mathieu functions. However, once the boundary becomes arbitrary this method is no longer applicable, and an alternative numerical solution

* Corresponding author. Tel.: +64 09 373 8768; fax: +64 09 373 7457.
E-mail addresses: m.smith@math.auckland.ac.nz (M.J. Smith), meylan@math.auckland.ac.nz (M.H. Meylan), ross@physics.usyd.edu.au (R.C. McPhedran).

0022-460X/$ - see front matter © 2011 Elsevier Ltd. All rights reserved.
doi:10.1016/j.jsv.2011.03.019

method must be developed. There exists a need to investigate more varied geometries for the case of a single cavity, which can open the way to studies of clusters and arrays of diverse cavities. In the context of solving the problem of water-wave scattering by polynya, Bennetts and Williams [11] solved the problem of water-wave scattering by an arbitrarily shaped cavity in a plate floating on water. They factorized the problem into a system of integral equations and expanded the boundary values in the Fourier series. The present work is closely based on their work, although they did not consider the phenomena of irregular frequencies.

It is well known that the solution for Helmholtz's equation by boundary integral equations leads to certain irregular frequencies, for which the matrices are ill-conditioned (Kleinman and Roach [12,13]). This phenomenon occurs in other boundary integral approaches, for example, in fluid/structure interactions (Linton and Mclver [14]). This ill-conditioning is a feature of the solution method, and it is associated with an interior eigenvalue problem. Various methods have been developed to control these irregular frequencies, and a popular method is the combined boundary integral equation method (CBIEM). This method involves overdetermining the standard system of integral equations with a modified system of integral equations evaluated at a series of field points taken to be inside the cavity region. This method was used by Lau and Hearn [15] to compute the added mass and damping coefficients for a three-dimensional wetted ship hull. Other methods for controlling ill-conditioning exist, including the null-field method outlined by Martin [16], and methods based on modifying the integral operator and its domain (Lau and Hearn [15]).

This paper presents a solution in the frequency domain for the problem of wave scattering by an infinite elastic thin plate with a cavity of arbitrary shape. The methods outlined in this paper have applications in ice sheet modelling, the development of offshore floating airports and other marine structures. There are also applications to problems in electrostatics involving non-circular, finitely conducting inclusions, and how the bulk properties of composite plates are affected by cavities, particularly by arrays of cavities (Yardley et al. [17], and Norris and Vemula [6]). The formulation outlined in this paper can easily incorporate more complicated shapes and boundary conditions, requiring only that the boundary be smooth. Cavities with wedges or corner points encounter the additional difficulty of hypersingular integral equations, which is discussed by Stern [18] but is not considered in the present work.

The outline of this paper is as follows. In Section 2, we formulate the problem in terms of a system of boundary integral equations (BIE), using the commutativity property of the biharmonic plate equation. In Section 3, we consider the most challenging case of free-edge conditions at the cavity edge, and derive a solution by expanding the unknowns in terms of the Fourier series. In Section 4, we show how the CBIEM approach can be used to control irregular frequencies. In Section 5, we give expressions for the solution outside the cavity, and Section 6 extends the formulation to other edge conditions. In Section 7, we consider the vibration of a plate of arbitrary geometry using our formulation, primarily as a check on our numerics. We give results in Section 8, beginning with a comparison with results previously computed for the vibration frequencies by Singh and Chakraverty [19–21] using Rayleigh–Ritz methods. While these Rayleigh–Ritz methods, especially those based on finite elements, have proved very effective for determining the frequencies of vibration, there might be situations where methods based on integral equations are preferable. Our results show generally good agreement with these previous estimates, which gives us a high level of confidence in the accuracy of our numerical solution. We then consider scattering by obstacles of various shapes. We give a brief summary in Section 9.

2. Problem formulation

We begin with the nondimensional elastic, thin-plate equation in the frequency domain given by

$$(\Delta^2-k^4)w=(\Delta+k^2)(\Delta-k^2)w=0, \tag{1}$$

where free-edge, clamped or simply-supported boundary conditions are imposed at the cavity edge and $k^2=\omega\sqrt{\rho h/D}$, where ω is the angular frequency, ρ is the mass density, h is the thickness and D is the flexural rigidity of the plate. We decompose the displacement of the plate w into incident and scattered components ($w = w^{\mathrm{I}}+w^{S}$), where w^{S} satisfies Sommerfeld's radiation condition, and for simplicity, we take a propagating incident plane wave $w^{\mathrm{I}}=\mathrm{e}^{ikr\cos\theta}$. As a matter of convention we let Ω denote the smooth cavity in our infinite plate with boundary $\partial\Omega$, and the region outside the cavity (occupied by the plate) is defined by Ω_∞ which has a boundary at infinity denoted by $\partial\Omega_\infty$ as shown in Fig. 1.

If we define $\Psi=(\Delta+k^2)w^{S}$ and $\Phi=(\Delta-k^2)w^{S}$, it is clear that Ψ satisfies the anti-Helmholtz equation

$$(\Delta-k^2)\Psi=0, \tag{2a}$$

and Φ satisfies the Helmholtz equation

$$(\Delta+k^2)\Phi=0. \tag{2b}$$

We define Green's identity

$$\int_{\partial\Omega}\{\phi(\mathbf{x}')\partial_{n'}G^{\mathrm{A,H}}(\mathbf{x},\mathbf{x}')-\partial_{n'}\phi(\mathbf{x}')G^{\mathrm{A,H}}(\mathbf{x},\mathbf{x}')\}\,\mathrm{d}S'=\begin{cases}\phi(\mathbf{x}) & \text{if } \mathbf{x}\in\Omega_\infty,\\ \frac{1}{2}\phi(\mathbf{x}) & \text{if } \mathbf{x}\in\partial\Omega,\\ 0 & \text{if } \mathbf{x}\in\Omega,\end{cases} \tag{3}$$

where G^{H} and G^{A} denote Green's functions for the Helmholtz and anti-Helmholtz equations, respectively (and ϕ, $G^{\mathrm{A,H}}$ satisfy the same differential equation and smoothness conditions specified in Kitahara [22]). We define these as

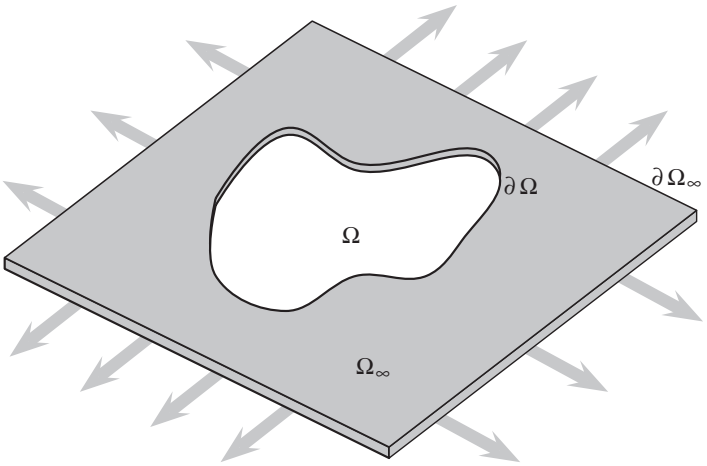

Fig. 1. Infinite plate with a cavity of arbitrary shape.

$G^{\mathrm{H}}(\mathbf{x},\mathbf{x}') = \frac{\mathrm{i}}{4}H_0^{(1)}(k|\mathbf{x}-\mathbf{x}'|)$ and $G^{\mathrm{A}}(\mathbf{x},\mathbf{x}') = \frac{\mathrm{i}}{4}H_0^{(1)}(\mathrm{i}k|\mathbf{x}-\mathbf{x}'|)$, where $H_0^{(1)}$ denotes a zero-order Hankel function of the first kind, with $\mathbf{x}$ and $\mathbf{x}'$ representing the field and source points, respectively.

Applying Green's identity to the Helmholtz and anti-Helmholtz expressions in (2a) and (2b) yields the system

$$\frac{1}{2}\Psi = \int_{\partial\Omega}\{\partial_{n'}G^{\mathrm{A}}\Psi - \partial_{n'}\Psi G^{\mathrm{A}}\}\,\mathrm{d}S', \tag{4a}$$

$$\frac{1}{2}\Phi = \int_{\partial\Omega}\{\partial_{n'}G^{\mathrm{H}}\Phi - \partial_{n'}\Phi G^{\mathrm{H}}\}\,\mathrm{d}S', \tag{4b}$$

where the integrals around the boundary at infinity $\partial\Omega_\infty$ disappear due to Sommerfeld's radiation condition. From this, our system can be expressed in terms of the scattered displacement directly

$$\frac{1}{2}(\Delta+k^2)w^{\mathrm{S}} = \int_{\partial\Omega}\{\partial_{n'}G^{\mathrm{A}}(\Delta+k^2)w^{\mathrm{S}} - \partial_{n'}(\Delta+k^2)w^{\mathrm{S}}G^{\mathrm{A}}\}\,\mathrm{d}S', \tag{5a}$$

$$\frac{1}{2}(\Delta-k^2)w^{\mathrm{S}} = \int_{\partial\Omega}\{\partial_{n'}G^{\mathrm{H}}(\Delta-k^2)w^{\mathrm{S}} - \partial_{n'}(\Delta-k^2)w^{\mathrm{S}}G^{\mathrm{H}}\}\,\mathrm{d}S'. \tag{5b}$$

After observing that $w^{\mathrm{S}} = w - w^{\mathrm{I}}$ and

$$(\Delta+k^2)w^{\mathrm{I}} = 0, \tag{6a}$$

$$(\Delta-k^2)w^{\mathrm{I}} = -2k^2w^{\mathrm{I}}. \tag{6b}$$

Eqs. (5a) and (5b) can then be expressed in terms of the total displacement

$$\frac{1}{2}(\Delta+k^2)w = \int_{\partial\Omega}\{\partial_{n'}G^{\mathrm{A}}(\Delta+k^2)w - \partial_{n'}(\Delta+k^2)wG^{\mathrm{A}}\}\,\mathrm{d}S', \tag{7a}$$

$$\frac{1}{2}(\Delta-k^2)w + k^2w^{\mathrm{I}} = \int_{\partial\Omega}\{\partial_{n'}G^{\mathrm{H}}(\Delta-k^2)w^{\mathrm{S}} - \partial_{n'}(\Delta-k^2)w^{\mathrm{S}}G^{\mathrm{H}}\}\,\mathrm{d}S' + 2k^2\int_{\partial\Omega}\{\partial_{n'}G^{\mathrm{H}}w^{\mathrm{I}} - \partial_{n'}w^{\mathrm{I}}G^{\mathrm{H}}\}\,\mathrm{d}S'. \tag{7b}$$

To evaluate the final integral in Eq. (7b), we apply Green's identity to the incident displacement alone, which yields an expression involving an integral around the boundary at infinity

$$\frac{1}{2}w^{\mathrm{I}} = \int_{\partial\Omega}\{\partial_{n'}G^{\mathrm{H}}w^{\mathrm{I}} - \partial_{n'}w^{\mathrm{I}}G^{\mathrm{H}}\}\,\mathrm{d}S' + \int_{\partial\Omega_\infty}\{\partial_{n'}G^{\mathrm{H}}w^{\mathrm{I}} - \partial_{n'}w^{\mathrm{I}}G^{\mathrm{H}}\}\,\mathrm{d}S', \tag{8}$$

where it can be shown from (3) that $\int_{\partial\Omega_\infty}\{\partial_{n'}G^{\mathrm{H}}w^{\mathrm{I}} - \partial_{n'}w^{\mathrm{I}}G^{\mathrm{H}}\}\mathrm{d}S' = w^{\mathrm{I}}$.

Consequently, the total plate displacement at the edge of the cavity can be expressed by the following system of boundary integral equations:

$$\frac{1}{2}(\Delta+k^2)w = \int_{\partial\Omega}\{\partial_{n'}G^{\mathrm{A}}(\Delta+k^2)w - \partial_{n'}(\Delta+k^2)wG^{\mathrm{A}}\}\,\mathrm{d}S', \tag{9a}$$

$$\frac{1}{2}(\Delta-k^2)w = -2k^2w^{\mathrm{I}} + \int_{\partial\Omega}\{\partial_{n'}G^{\mathrm{H}}(\Delta-k^2)w - \partial_{n'}(\Delta-k^2)wG^{\mathrm{H}}\}\,\mathrm{d}S'. \tag{9b}$$

These equations will be the basis of our numerical solution for computing the plate displacement. This expression extends the boundary integral equation method for Helmholtz's equation to the biharmonic plate equation.

3. Free-edge boundary conditions

The free-edge boundary conditions for a smooth cavity can be represented in the form

$$\Delta w = \beta(\partial_s^2 + \partial_s\Theta\partial_n)w, \tag{10a}$$

$$\partial_{n'}\Delta w = \beta(\partial_s^2\Theta\partial_s + \partial_s\Theta\partial_s^2 - \partial_s^2\partial_n)w, \tag{10b}$$

(Stern [18]) where $\partial_s = \nabla\cdot\mathbf{s}$, $\partial_n = \nabla\cdot\mathbf{n}$, $\mathbf{s}$ is unit tangential to $\partial\Omega$, $\mathbf{n}$ and $\mathbf{n}'$ denote unit normal vectors to $\partial\Omega$ (with respect to the field and source points, respectively), and $\beta = 1-\nu$, where ν is the Poisson ratio of the plate. We introduce the notation $\Theta = \Theta(s)$ for the direction cosine such that $\mathbf{n} = (\cos\Theta,\sin\Theta)$. We also assume that the cavity boundary $\partial\Omega$ is parametrized by s such that $s\in(-\gamma,\gamma)$, using the notation s and s' when referring to the field and source points, respectively.

In a manner identical to Bennetts and Williams [11], for the case of free-edge conditions, we expand the resulting two unknowns (the displacement and the normal derivative of the displacement) in Eqs. (9a) and (9b) in terms of the following Fourier series:

$$w = \sum_{m=-\infty}^{\infty} c_m e^{im\pi s'/\gamma}, \quad \partial_{n'}w = \sum_{m=-\infty}^{\infty} d_m e^{im\pi s'/\gamma}, \tag{11}$$

and then apply the relevant boundary conditions.

Implementing the Fourier series above allows Eqs. (9a) and (9b) to take the form

$$\begin{aligned}\sum_{m=-\infty}^{\infty}\left\{\frac{1}{2}[k^2-\beta(m\pi/\gamma)^2]e^{im\pi s/\gamma}\right\}c_m + \left\{\frac{1}{2}\beta\partial_s\Theta(s)e^{im\pi s/\gamma}\right\}d_m = \sum_{m=-\infty}^{\infty} c_m\Bigg\{&[k^2-\beta(m\pi/\gamma)^2]\int_{\partial\Omega}\partial_{n'}G^{\mathrm{A}}e^{im\pi s'/\gamma}\,dS'\\ &+\beta(m\pi/\gamma)^2\int_{\partial\Omega}\partial_{s'}\Theta(s')G^{\mathrm{A}}e^{im\pi s'/\gamma}\,dS' - im\beta\pi/\gamma\int_{\partial\Omega}\partial_{s'}^2\Theta(s')G^{\mathrm{A}}e^{im\pi s'/\gamma}\,dS'\Bigg\}\\ &+d_m\Bigg\{\beta\int_{\partial\Omega}\partial_{s'}\Theta(s')\partial_{n'}G^{\mathrm{A}}e^{im\pi s'/\gamma}\,dS' - [k^2+\beta(m\pi/\gamma)^2]\int_{\partial\Omega}G^{\mathrm{A}}e^{im\pi s'/\gamma}\,dS'\Bigg\},\end{aligned} \tag{12a}$$

and

$$\begin{aligned}\sum_{m=-\infty}^{\infty}\left\{\frac{1}{2}\beta\partial_s\Theta(s)e^{im\pi s/\gamma}\right\}d_m - \left\{\frac{1}{2}[k^2+\beta(m\pi/\gamma)^2]e^{im\pi s/\gamma}\right\}c_m = -2k^2w^{\mathrm{I}} + \sum_{m=-\infty}^{\infty} c_m\Bigg\{&-[k^2+\beta(m\pi/\gamma)^2]\int_{\partial\Omega}\partial_{n'}G^{\mathrm{H}}e^{im\pi s'/\gamma}\,dS'\\ &+\beta(m\pi/\gamma)^2\int_{\partial\Omega}\partial_{s'}\Theta(s')G^{\mathrm{H}}e^{im\pi s'/\gamma}\,dS' - im\beta\pi/\gamma\int_{\partial\Omega}\partial_{s'}^2\Theta(s')G^{\mathrm{H}}e^{im\pi s'/\gamma}\,dS'\Bigg\}\\ &+d_m\Bigg\{\beta\int_{\partial\Omega}\partial_{s'}\Theta(s')\partial_{n'}G^{\mathrm{H}}e^{im\pi s'/\gamma}\,dS' + [k^2-\beta(m\pi/\gamma)^2]\int_{\partial\Omega}G^{\mathrm{H}}e^{im\pi s'/\gamma}\,dS'\Bigg\}.\end{aligned} \tag{12b}$$

Multiplying these resulting expressions by $e^{in\pi s/\gamma}$, truncating the Fourier series, and integrating over the cavity boundary $\partial\Omega$ with respect to the field point yields the block-matrix system:

$$\mathbf{M}\mathbf{z} = \left[\begin{array}{c|c}\mathbf{M}_{11} & \mathbf{M}_{12}\\ \hline \mathbf{M}_{21} & \mathbf{M}_{22}\end{array}\right]\mathbf{z} = \mathbf{f}, \tag{13}$$

with the component blocks of $\mathbf{M}$ defined as

$$\mathbf{M}_{11} = [\tfrac{1}{2}(k^2\mathbf{I}-\eta\mathbf{N}^2)\mathbf{G} + \xi\mathbf{N}\mathbf{B}^{\mathrm{A}} - \eta\mathbf{N}^2\mathbf{A}^{\mathrm{A}} - (k^2\mathbf{I}-\eta\mathbf{N}^2)\mathbf{E}^{\mathrm{A}}], \tag{14a}$$

$$\mathbf{M}_{12} = [\tfrac{1}{2}\beta\mathbf{H} - \beta\mathbf{C}^{\mathrm{A}} + (k^2\mathbf{I}+\eta\mathbf{N}^2)\mathbf{D}^{\mathrm{A}}], \tag{14b}$$

$$\mathbf{M}_{21} = [(k^2\mathbf{I}+\eta\mathbf{N}^2)\mathbf{E}^{\mathrm{H}} + \xi\mathbf{N}\mathbf{B}^{\mathrm{H}} - \eta\mathbf{N}^2\mathbf{A}^{\mathrm{H}} - \tfrac{1}{2}(k^2\mathbf{I}+\eta\mathbf{N}^2)\mathbf{G}], \tag{14c}$$

$$\mathbf{M}_{22} = [\tfrac{1}{2}\beta\mathbf{H} - \beta\mathbf{C}^{\mathrm{H}} - (k^2\mathbf{I}-\eta\mathbf{N}^2)\mathbf{D}^{\mathrm{H}}], \tag{14d}$$

where $\mathbf{I}$ denotes the identity matrix, $\mathbf{z} = [c_M,\ldots,c_{-M},d_M,\ldots,d_{-M}]^{\mathrm{T}}$, $\mathbf{f} = [\mathbf{0},\mathbf{g}]^{\mathrm{T}}$, $\xi = i\beta\pi/\gamma$, $\eta = \beta\pi^2/\gamma^2$,

$$\mathbf{A}_{mn}^{\mathrm{A,H}} = \int_{\partial\Omega}\int_{\partial\Omega}\partial_{s'}\Theta(s')G^{\mathrm{A,H}}e^{im\pi s'/\gamma}e^{in\pi s/\gamma}\,dS'\,dS, \quad \mathbf{G}_{mn} = \int_{\partial\Omega}e^{i(m+n)\pi s/\gamma}\,dS,$$

$$\mathbf{B}_{mn}^{\mathrm{A,H}} = \int_{\partial\Omega}\int_{\partial\Omega}\partial_{s'}^2\Theta(s')G^{\mathrm{A,H}}e^{im\pi s'/\gamma}e^{in\pi s/\gamma}\,dS'\,dS, \quad \mathbf{H}_{mn} = \int_{\partial\Omega}\partial_s\Theta(s)e^{i(m+n)\pi s/\gamma}\,dS,$$

$$\mathbf{C}_{mn}^{\mathrm{A,H}} = \int_{\partial\Omega}\int_{\partial\Omega}\partial_{s'}\Theta(s')\partial_{n'}G^{\mathrm{A,H}}e^{im\pi s'/\gamma}e^{in\pi s/\gamma}\,dS'\,dS, \quad \mathbf{N}_{mn} = n\delta_{mn},$$

$$\mathbf{D}^{\mathrm{A,H}}_{mn} = \int_{\partial\Omega}\int_{\partial\Omega} G^{\mathrm{A,H}} \mathrm{e}^{\mathrm{i}m\pi s'/\gamma}\mathrm{e}^{\mathrm{i}n\pi s/\gamma}\,\mathrm{d}S'\,\mathrm{d}S, \quad \mathbf{g}_n = -2k^2\int_{\partial\Omega} w^{\mathrm{I}}\mathrm{e}^{\mathrm{i}n\pi s/\gamma}\,\mathrm{d}S, \quad \text{and}$$

$$\mathbf{E}^{\mathrm{A,H}}_{mn} = \int_{\partial\Omega}\int_{\partial\Omega} \partial_{n'} G^{\mathrm{A,H}} \mathrm{e}^{\mathrm{i}m\pi s'/\gamma}\mathrm{e}^{\mathrm{i}n\pi s/\gamma}\,\mathrm{d}S'\,\mathrm{d}S.$$

Note that in the definitions above, if the superscript A used, then the anti-Helmholtz Green's function G^{A} is used to compute the matrix. Similarly, if the superscript H is used, then the Helmholtz Green's function G^{H} is used, for example,

$$\mathbf{A}^{\mathrm{A}}_{mn} = \int_{\partial\Omega}\int_{\partial\Omega} \partial_{s'}\Theta(s') G^{\mathrm{A}} \mathrm{e}^{\mathrm{i}m\pi s'/\gamma}\mathrm{e}^{\mathrm{i}n\pi s/\gamma}\,\mathrm{d}S'\,\mathrm{d}S.$$

As is the case for Helmholtz's equation, for certain frequencies k the matrix $\mathbf{M}$ is non-invertible, giving rise to problems with ill-conditioning. The control of this phenomenon is the subject of the following section.

4. Combined boundary integral equation method

In order to numerically control ill-conditioning we apply the technique as discussed by Lau and Hearn [15], which is known as the combined boundary integral equation method (CBIEM). This technique involves overdetermining our existing system of equations by positioning the field point inside the cavity Ω, with each point (denoted by $\hat{\mathbf{p}}_j$) giving rise to an additional set of integral equations denoted by

$$0 = \int_{\partial\Omega} \{\partial_{n'} G^{\mathrm{A}}(\hat{\mathbf{p}}_j,\mathbf{x}')(\Delta+k^2)w - \partial_{n'}(\Delta+k^2)wG^{\mathrm{A}}(\hat{\mathbf{p}}_j,\mathbf{x}')\}\,\mathrm{d}S', \tag{15a}$$

$$2k^2 w^{\mathrm{I}}(\hat{\mathbf{p}}_j) = \int_{\partial\Omega} \{\partial_{n'} G^{\mathrm{H}}(\hat{\mathbf{p}}_j,\mathbf{x}')(\Delta-k^2)w - \partial_{n'}(\Delta-k^2)wG^{\mathrm{H}}(\hat{\mathbf{p}}_j,\mathbf{x}')\}\,\mathrm{d}S'. \tag{15b}$$

The position of these points is important as they must not coincide with the nodal points of interior eigenfunctions, and these are unknown in general (Lau and Hearn [15]). To overcome this, we sample our field points from a ball of small (but not too small) radius centred about the origin. Another ill-conditioned problem is encountered if the ball is too small, as only the zero-order Bessel functions will contribute towards controlling ill-conditioning. Likewise, if the radius is too big and we sample field points that are too close to the boundary, then we encounter problems in connection with Green's identity (3).

The location of these resonant wavenumbers is also unknown *a priori* in general, and correspond to the eigenvalues of an interior problem whose boundary conditions are unknown, with the added difficulty that these adjoint conditions do not relate to a physical problem. Unfortunately, there is no simple connection as in Helmholtz's equation, where an external Dirichlet problem has irregular frequencies corresponding to the eigensolutions of the corresponding internal Neumann problem, and vice-versa (Kleinman and Roach [12]).

Implementing the free-edge boundary conditions and truncating the Fourier series expansions (11), in an approach similar to that followed in the previous section, gives rise to the CBIEM system for the point $\hat{\mathbf{p}}_j$

$$\hat{\mathbf{M}}_j\mathbf{z} = \hat{\mathbf{f}}_j, \tag{16}$$

where

$$\hat{\mathbf{M}}_j = \left[\begin{array}{c|c} (k^2\mathbf{I}-\eta\mathbf{N}^2)\hat{\mathbf{H}}^j + \eta\mathbf{N}^2\hat{\mathbf{A}}^j - \xi\mathbf{N}\hat{\mathbf{B}}^j & \beta\hat{\mathbf{C}}^j - (k^2\mathbf{I}+\eta\mathbf{N}^2)\hat{\mathbf{J}}^j \\ \hline \eta\mathbf{N}^2\hat{\mathbf{D}}^j - \xi\mathbf{N}\hat{\mathbf{E}}^j - (k^2\mathbf{I}+\eta\mathbf{N}^2)\hat{\mathbf{L}}^j & \beta\hat{\mathbf{G}}^j + (k^2\mathbf{I}-\eta\mathbf{N}^2)\hat{\mathbf{K}}^j \end{array}\right], \tag{17}$$

with $\hat{\mathbf{f}} = [0,\hat{g}]^{\mathrm{T}}$, $\hat{g} = 2k^2 w^{\mathrm{I}}(\hat{\mathbf{p}}_j)$, and

$$\hat{\mathbf{A}}^j_m = \int_{\partial\Omega} \partial_{s'}\Theta(s') G^{\mathrm{A}}(\hat{\mathbf{p}}_j,\mathbf{x}')\mathrm{e}^{\mathrm{i}m\pi s'/\gamma}\,\mathrm{d}S', \quad \hat{\mathbf{G}}^j_m = \int_{\partial\Omega} \partial_{s'}\Theta(s')\partial_{n'} G^{\mathrm{H}}(\hat{\mathbf{p}}_j,\mathbf{x}')\mathrm{e}^{\mathrm{i}m\pi s'/\gamma}\,\mathrm{d}S',$$

$$\hat{\mathbf{B}}^j_m = \int_{\partial\Omega} \partial^2_{s'}\Theta(s') G^{\mathrm{A}}(\hat{\mathbf{p}}_j,\mathbf{x}')\mathrm{e}^{\mathrm{i}m\pi s'/\gamma}\,\mathrm{d}S', \quad \hat{\mathbf{H}}^j_m = \int_{\partial\Omega} \partial_{n'} G^{\mathrm{A}}(\hat{\mathbf{p}}_j,\mathbf{x}')\mathrm{e}^{\mathrm{i}m\pi s'/\gamma}\,\mathrm{d}S',$$

$$\hat{\mathbf{C}}^j_m = \int_{\partial\Omega} \partial_{s'}\Theta(s')\partial_{n'} G^{\mathrm{A}}(\hat{\mathbf{p}}_j,\mathbf{x}')\mathrm{e}^{\mathrm{i}m\pi s'/\gamma}\,\mathrm{d}S', \quad \hat{\mathbf{J}}^j_m = \int_{\partial\Omega} G^{\mathrm{A}}(\hat{\mathbf{p}}_j,\mathbf{x}')\mathrm{e}^{\mathrm{i}m\pi s'/\gamma}\,\mathrm{d}S',$$

$$\hat{\mathbf{D}}^j_m = \int_{\partial\Omega} \partial_{s'}\Theta(s') G^{\mathrm{H}}(\hat{\mathbf{p}}_j,\mathbf{x}')\mathrm{e}^{\mathrm{i}m\pi s'/\gamma}\,\mathrm{d}S', \quad \hat{\mathbf{K}}^j_m = \int_{\partial\Omega} G^{\mathrm{H}}(\hat{\mathbf{p}}_j,\mathbf{x}')\mathrm{e}^{\mathrm{i}m\pi s'/\gamma}\,\mathrm{d}S',$$

$$\hat{\mathbf{E}}^j_m = \int_{\partial\Omega} \partial^2_{s'}\Theta(s') G^{\mathrm{H}}(\hat{\mathbf{p}}_j,\mathbf{x}')\mathrm{e}^{\mathrm{i}m\pi s'/\gamma}\,\mathrm{d}S', \quad \hat{\mathbf{L}}^j_m = \int_{\partial\Omega} \partial_{n'} G^{\mathrm{H}}(\hat{\mathbf{p}}_j,\mathbf{x}')\mathrm{e}^{\mathrm{i}m\pi s'/\gamma}\,\mathrm{d}S'.$$

Incorporating the CBIEM system(s) with our standard system gives the overdetermined problem

$$\tilde{\mathbf{M}}\mathbf{z}=\begin{bmatrix}\mathbf{M}\\ \hat{\mathbf{M}}_1\\ \hat{\mathbf{M}}_2\\ \vdots\end{bmatrix}\mathbf{z}=\begin{bmatrix}\mathbf{f}\\ \hat{\mathbf{f}}_1\\ \hat{\mathbf{f}}_2\\ \vdots\end{bmatrix}=\tilde{\mathbf{f}}, \tag{18}$$

which can be solved by using a standard Moore–Penrose generalized inverse. This solution controls irregular frequency effects, provided that $\tilde{\mathbf{f}}\in\mathrm{col}(\tilde{\mathbf{M}})$.

5. Solution outside of cavity boundary

Using the solution for the two unknowns at the cavity edge $\partial\Omega$, the displacement of the plate for a point in the exterior region Ω_∞ can be computed. This is achieved in general by combining Eqs. (9a) and (9b) to obtain

$$w(\mathbf{x})=w^{\mathrm{I}}(\mathbf{x})-\int_{\partial\Omega}\{\partial_{n'}G^{\mathrm{P}}(\mathbf{x},\mathbf{x}')(\Delta-k^2)w(\mathbf{x}')-\partial_{n'}(\Delta-k^2)w(\mathbf{x}')G^{\mathrm{P}}(\mathbf{x},\mathbf{x}')\}\,\mathrm{d}S'+\int_{\partial\Omega}\{\partial_{n'}G^{\mathrm{A}}(\mathbf{x},\mathbf{x}')w(\mathbf{x}')-\partial_{n'}w(\mathbf{x}')G^{\mathrm{A}}(\mathbf{x},\mathbf{x}')\}\,\mathrm{d}S', \tag{19}$$

where

$$G^{\mathrm{P}}(\mathbf{x},\mathbf{x}')=\frac{1}{2k^2}[G^{\mathrm{H}}(\mathbf{x},\mathbf{x}')-G^{\mathrm{A}}(\mathbf{x},\mathbf{x}')]=\frac{\mathrm{i}}{8k^2}[H_0^{(1)}(k|\mathbf{x}-\mathbf{x}'|)-H_0^{(1)}(\mathrm{i}k|\mathbf{x}-\mathbf{x}'|)], \tag{20}$$

is Green's function which satisfies the nondimensional plate equation given by

$$(\Delta^2-k^4)G^{\mathrm{P}}(\mathbf{x},\mathbf{x}')=\delta(\mathbf{x}-\mathbf{x}'), \tag{21}$$

(Norris and Vemula [6]). Substituting the boundary conditions (10a) and (10b) into expression (19) allows us to compute the displacement of the plate in Ω_∞ for the case of a free-edge cavity

$$\begin{aligned}w(\mathbf{x})=w^{\mathrm{I}}(\mathbf{x})&-\int_{\partial\Omega}\{\partial_{n'}G^{\mathrm{P}}(\mathbf{x},\mathbf{x}')[\beta\partial_{s'}^2-k^2]w(\mathbf{x}')-\beta[\partial_{s'}^2\Theta\partial_{s'}+\partial_{s'}\Theta\partial_{s'}^2]w(\mathbf{x}')G^{\mathrm{P}}(\mathbf{x},\mathbf{x}')\}\,\mathrm{d}S'\\ -\int_{\partial\Omega}\{\partial_{n'}G^{\mathrm{P}}(\mathbf{x},\mathbf{x}')[\beta\partial_{s'}\Theta]\partial_{n'}w(\mathbf{x}')&+[\beta\partial_{s'}^2+k^2]\partial_{n'}w(\mathbf{x}')G^{\mathrm{P}}(\mathbf{x},\mathbf{x}')\}\,\mathrm{d}S'+\int_{\partial\Omega}\{\partial_{n'}G^{\mathrm{A}}(\mathbf{x},\mathbf{x}')w(\mathbf{x}')-\partial_{n'}w(\mathbf{x}')G^{\mathrm{A}}(\mathbf{x},\mathbf{x}')\}\,\mathrm{d}S'.\end{aligned} \tag{22}$$

6. Other boundary conditions

One advantage of formulating this problem in terms of boundary integral equations is that different boundary conditions can be easily considered and implemented (although the free-edge case is the most challenging). This includes clamped boundary conditions given by

$$w=0,\quad \partial_{n'}w=0. \tag{23}$$

Applying these conditions to Eqs. (9a) and (9b), and expanding $\Delta w=\sum c_m\mathrm{e}^{\mathrm{i}m\pi s'/\gamma}$, and $\partial_{n'}\Delta w=\sum d_m\mathrm{e}^{\mathrm{i}m\pi s'/\gamma}$ admits a system of equations similar to expressions (13) and (16) except that

$$\mathbf{M}=\left[\begin{array}{c|c}\frac{1}{2}\mathbf{G}-\mathbf{E}^{\mathrm{A}} & \mathbf{D}^{\mathrm{A}}\\ \hline \frac{1}{2}\mathbf{G}-\mathbf{E}^{\mathrm{H}} & \mathbf{D}^{\mathrm{H}}\end{array}\right],\quad \hat{\mathbf{M}}_j=\left[\begin{array}{c|c}\hat{\mathbf{H}}^j & -\hat{\mathbf{J}}^j\\ \hline \hat{\mathbf{L}}^j & -\hat{\mathbf{K}}^j\end{array}\right]. \tag{24}$$

Note that for clamped boundary conditions, a Fourier series expansion for the unknowns Δw and $\partial_{n'}\Delta w$ is not actually required (as there are no tangential derivative terms present in the boundary conditions), but it is introduced for clarifying the equations.

The plate displacement in Ω_∞ is computed in a manner similar to the free-edge case, and it is given by

$$w(\mathbf{x})=w^{\mathrm{I}}(\mathbf{x})-\int_{\partial\Omega}\{\partial_{n'}G^{\mathrm{P}}(\mathbf{x},\mathbf{x}')\Delta w(\mathbf{x}')-\partial_{n'}\Delta w(\mathbf{x}')G^{\mathrm{P}}(\mathbf{x},\mathbf{x}')\}\,\mathrm{d}S'. \tag{25}$$

For the case of a smooth boundary, applying the simply-supported boundary conditions given by

$$w=0,\quad \Delta w-\beta\partial_s\Theta\partial_n w=0, \tag{26}$$

in a manner similar to before, it can be shown that

$$\mathbf{M}=\left[\begin{array}{c|c}\mathbf{D}^{\mathrm{A}} & \frac{1}{2}\beta\mathbf{H}-\beta\mathbf{C}^{\mathrm{A}}+k^2\mathbf{D}^{\mathrm{A}}\\ \hline \mathbf{D}^{\mathrm{H}} & \frac{1}{2}\beta\mathbf{H}-\beta\mathbf{C}^{\mathrm{H}}-k^2\mathbf{D}^{\mathrm{H}}\end{array}\right],\quad \hat{\mathbf{M}}_j=\left[\begin{array}{c|c}-\hat{\mathbf{J}}^j & \beta\hat{\mathbf{C}}^j-k^2\hat{\mathbf{J}}^j\\ \hline -\hat{\mathbf{K}}^j & \beta\hat{\mathbf{G}}^j+k^2\hat{\mathbf{K}}^j\end{array}\right], \tag{27}$$

where $\partial_{n'}\Delta w = \sum c_m e^{im\pi s'/\gamma}$ and $\partial_{n'} w = \sum d_m e^{im\pi s'/\gamma}$, with the plate displacement in Ω_∞ given by

$$w(\mathbf{x}) = w^{\mathrm{I}}(\mathbf{x}) - \int_{\partial\Omega} \{[\beta\partial_{s'}\Theta\partial_{n'}G^{\mathrm{P}}(\mathbf{x},\mathbf{x}') + G^{\mathrm{A}}(\mathbf{x},\mathbf{x}') + k^2 G^{\mathrm{P}}]\partial_{n'} w(\mathbf{x}')\}\, \mathrm{d}S' + \int_{\partial\Omega} \{G^{\mathrm{P}}(\mathbf{x},\mathbf{x}')\partial_{n'}\Delta w(\mathbf{x}')\}\, \mathrm{d}S'. \tag{28}$$

7. Arbitrary finite plate vibration problem

Previously we considered the problem of wave scattering in an infinite plate with a closed cavity. A connection is now established between the solution method for this problem and the vibration problem of a finite plate surrounded by a vacuum. This second problem is shown in Fig. 2.

Formulating the finite plate vibration problem in terms of a system of boundary integral equations yields a system identical to Eqs. (9a) and (9b), except that there is no incident displacement term present. However, in order to relate this system in terms of the vibration problem, we need to reorient the normal derivative and look closely at single-layer distribution terms present in our integral equations, taking note that there is a jump discontinuity at the boundary given by

$$\lim_{\mathbf{x}\to\mathbf{x}^-} \int_{\partial\Omega} w(\mathbf{x}')\partial_{n'}G(\mathbf{x},\mathbf{x}')\, \mathrm{d}S' = w(\mathbf{x}) + \int_{\partial\Omega} w(\mathbf{x}')\partial_{n'}G(\mathbf{x},\mathbf{x}')\, \mathrm{d}S', \tag{29}$$

where $\mathbf{x}\to\mathbf{x}^-$ denotes the field point approaching the boundary from the interior region Ω, Kleinman and Roach [13]. Note that the normal derivative in the final integral of equation (29) must be suitably oriented.

Consequently, the boundary integral system for computing the vibration of a finite plate is given in general by

$$-\frac{1}{2}(\Delta + k^2)w = \int_{\partial\Omega} \{\partial_{n'}G^{\mathrm{A}}(\Delta + k^2)w + \partial_{n'}(\Delta + k^2)wG^{\mathrm{A}}\}\, \mathrm{d}S', \tag{30a}$$

$$-\frac{1}{2}(\Delta - k^2)w = \int_{\partial\Omega} \{\partial_{n'}G^{\mathrm{H}}(\Delta - k^2)w + \partial_{n'}(\Delta - k^2)wG^{\mathrm{H}}\}\, \mathrm{d}S'. \tag{30b}$$

If we implement the reoriented free-edge boundary conditions given by

$$\Delta w = \beta(\partial_s^2 - \partial_s\Theta\partial_n)w, \tag{31a}$$

$$\partial_{n'}\Delta w = -\beta(\partial_s^2\Theta\partial_s + \partial_s\Theta\partial_s^2 + \partial_s^2\partial_n)w, \tag{31b}$$

use the series expansion given by Eq. (11), multiply by $e^{in\pi s/\gamma}$ and integrate over the cavity edge $\partial\Omega$ with respect to the field point, we obtain the following block-matrix system:

$$\mathbf{P}(k)\mathbf{z} = \left[\begin{array}{c|c} \mathbf{P}_{11} & \mathbf{P}_{12} \\ \hline \mathbf{P}_{21} & \mathbf{P}_{22} \end{array}\right]\mathbf{z} = \mathbf{0}, \tag{32}$$

where

$$\mathbf{P}_{11} = [\tfrac{1}{2}(\eta\mathbf{N}^2 - k^2\mathbf{I})\mathbf{G} - (k^2\mathbf{I} - \eta\mathbf{N}^2)\mathbf{E}^{\mathrm{A}} + \xi\mathbf{N}\mathbf{B}^{\mathrm{A}} - \eta\mathbf{N}^2\mathbf{A}^{\mathrm{A}}], \tag{33a}$$

$$\mathbf{P}_{12} = [\tfrac{1}{2}\beta\mathbf{H} + \beta\mathbf{C}^{\mathrm{A}} - (k^2\mathbf{I} + \eta\mathbf{N}^2)\mathbf{D}^{\mathrm{A}}], \tag{33b}$$

$$\mathbf{P}_{21} = [\tfrac{1}{2}(\eta\mathbf{N}^2 + k^2\mathbf{I})\mathbf{G} + (k^2\mathbf{I} + \eta\mathbf{N}^2)\mathbf{E}^{\mathrm{H}} + \xi\mathbf{N}\mathbf{B}^{\mathrm{H}} - \eta\mathbf{N}^2\mathbf{A}^{\mathrm{H}}], \tag{33c}$$

$$\mathbf{P}_{22} = [\tfrac{1}{2}\beta\mathbf{H} + \beta\mathbf{C}^{\mathrm{H}} + (k^2\mathbf{I} - \eta\mathbf{N}^2)\mathbf{D}^{\mathrm{H}}]. \tag{33d}$$

The vibration frequencies of an arbitrary plate are denoted by $\mu_l = k_l^2$, where k_l corresponds to the values of k such that $\mathbf{P}(k)$ has zero eigenvalue. It is important to note that these eigenvalues do not correspond to the irregular frequencies for the external cavity problem with free-edge, simply-supported or clamped boundary conditions. That is, the irregular frequencies do not match numerically with the vibration frequencies, and they do not correspond to a physical problem, Burton and Miller [23]. If these values were known, then techniques to control ill-conditioning would only need to be applied in the neighbourhood of each irregular frequency.

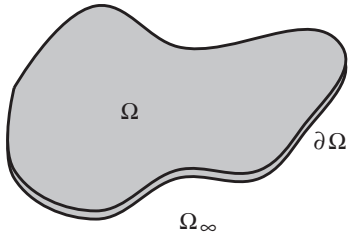

Fig. 2. Vibration of an arbitrarily shaped smooth plate.

For clamped boundary conditions (which are unchanged when considering the vibration problem) we obtain a system similar to (32), except that

$$\mathbf{P}(k)=\left[\begin{array}{c|c}\frac{1}{2}\mathbf{G}+\mathbf{E}^{\mathrm{A}} & \mathbf{D}^{\mathrm{A}}\\ \hline \frac{1}{2}\mathbf{G}+\mathbf{E}^{\mathrm{H}} & \mathbf{D}^{\mathrm{H}}\end{array}\right]. \tag{34}$$

For simply-supported boundary conditions, after adjusting the normal derivative for the vibration problem, we obtain

$$w=0,\quad \Delta w=-\beta\partial_s\Theta\partial_n w, \tag{35}$$

which admits the system in (32), where

$$\mathbf{P}(k)=\left[\begin{array}{c|c}-\mathbf{D}^{\mathrm{A}} & \frac{1}{2}\beta\mathbf{H}-k^2\mathbf{D}^{\mathrm{A}}+\beta\mathbf{C}^{\mathrm{A}}\\ \hline -\mathbf{D}^{\mathrm{H}} & \frac{1}{2}\beta\mathbf{H}+k^2\mathbf{D}^{\mathrm{H}}+\beta\mathbf{C}^{\mathrm{H}}\end{array}\right]. \tag{36}$$

7.1. Computing the frequencies of vibration

The standard method used to determine vibration frequencies is finite-element methods (FEM); however, in this paper values are computed using a first-order expansion of $\mathbf{P}(k)$, giving rise to a generalized eigenvalue problem for the update κ based on an initial estimate k_0 as follows:

$$\mathbf{P}(k_0)\mathbf{z}=-\kappa\mathbf{P}'(k_0)\mathbf{z}\quad\text{where } \kappa=k-k_0, \tag{37}$$

where the update is given by the real part of the minimum eigenvalue $|\kappa|$ for the system (as k is real).

If we compute the derivative of $\mathbf{P}(k_0)$ using a finite difference method we can obtain the expression

$$\mathbf{P}'(k_0)=\frac{1}{2\Delta k_0}[\mathbf{P}(k_0+\Delta k_0)-\mathbf{P}(k_0-\Delta k_0)], \tag{38}$$

where Δk_0 denotes a small change in k_0. However, if Δk_0 is too small, then the elements of $\mathbf{P}'(k_0)$ become large (due to the $1/2\Delta k_0$ term), giving rise to an ill-conditioned matrix. In such a case, this method becomes highly sensitive to the initial estimate for the vibration frequency, with convergence issues arising unless the initial estimate is suitably close to the real root. In general, accuracy for this method may only be valid to a few decimal places. This method is proposed primarily to confirm the results obtained by Singh and Chakraverty [19–21], using their values as a starting point for the algorithm. We do not claim that this is the best method to find the frequencies of vibration, but it might prove useful in certain situations. Nevertheless, calculation of these vibration frequencies acts as a very useful check of our numerical code.

7.2. Computing the displacement of the plate

Having solved the eigenvalue problem given by Eq. (32) we take the eigenvector of $\mathbf{P}(k)$ that corresponds to the eigenvalue numerically closest to zero. This eigenvector corresponds to a vector of coefficients $\mathbf{z}$, which is then used to compute the two appropriate unknowns at the plate edge by using the series expansions given in (11).

The expression for the plate displacement here is found in a manner identical to that for the cavity problem. By combining Eqs. (30a) and (30b) we can achieve in general

$$w(\mathbf{x})=2\int_{\partial\Omega}\{\partial_{n'}G^{\mathrm{P}}(\mathbf{x},\mathbf{x}')\Delta w(\mathbf{x}')+\partial_{n'}\Delta w(\mathbf{x}')G^{\mathrm{P}}(\mathbf{x},\mathbf{x}')\}\,\mathrm{d}S'-\int_{\partial\Omega}\{[\partial_{n'}G^{\mathrm{A}}(\mathbf{x},\mathbf{x}')+\partial_{n'}G^{\mathrm{H}}(\mathbf{x},\mathbf{x}')]w(\mathbf{x}')+\partial_{n'}w(\mathbf{x}')[G^{\mathrm{A}}(\mathbf{x},\mathbf{x}')+G^{\mathrm{H}}(\mathbf{x},\mathbf{x}')]\}\,\mathrm{d}S', \tag{39}$$

for the displacement of the plate.

Substituting the boundary conditions (31a) and (31b) into expression (39) allows us to compute the displacement of the plate for the case of free-edge boundary conditions

$$\begin{aligned}w(\mathbf{x})=2\beta\int_{\partial\Omega}\{&[\partial_{n'}G^{\mathrm{P}}(\mathbf{x},\mathbf{x}')\partial_{s'}^2-G^{\mathrm{P}}(\mathbf{x},\mathbf{x}')(\partial_{s'}^2\Theta\partial_{s'}+\partial_{s'}\Theta\partial_{s'}^2)]w(\mathbf{x}')-[\partial_{n'}G^{\mathrm{P}}(\mathbf{x},\mathbf{x}')\partial_{s'}\Theta\\ &+G^{\mathrm{P}}(\mathbf{x},\mathbf{x}')\partial_{s'}^2]\partial_{n'}w(\mathbf{x})\}\,dS'-\int_{\partial\Omega}\{[\partial_{n'}G^{\mathrm{A}}(\mathbf{x},\mathbf{x}')+\partial_{n'}G^{\mathrm{H}}(\mathbf{x},\mathbf{x}')]w(\mathbf{x}')+\partial_{n'}w(\mathbf{x}')[G^{\mathrm{A}}(\mathbf{x},\mathbf{x}')+G^{\mathrm{H}}(\mathbf{x},\mathbf{x}')]\}\,\mathrm{d}S'.\end{aligned} \tag{40}$$

Similarly for clamped boundary conditions which are given by (35) we obtain

$$w(\mathbf{x})=2\int_{\partial\Omega}\{\partial_{n'}G^{\mathrm{P}}(\mathbf{x},\mathbf{x}')\Delta w(\mathbf{x}')+\partial_{n'}\Delta w(\mathbf{x}')G^{\mathrm{P}}(\mathbf{x},\mathbf{x}')\}\,\mathrm{d}S', \tag{41}$$

and for simply-supported boundary conditions, which are given by (23), it can be shown that

$$w(\mathbf{x})=2\int_{\partial\Omega}\{G^{\mathrm{P}}(\mathbf{x},\mathbf{x}')\partial_{n'}\Delta w(\mathbf{x}')-[\beta\partial_{s'}\Theta\partial_{n'}G^{\mathrm{P}}(\mathbf{x},\mathbf{x}')]\partial_{n'}w(\mathbf{x}')\}\,\mathrm{d}S'-\int_{\partial\Omega}\{\partial_{n'}w(\mathbf{x}')[G^{\mathrm{A}}(\mathbf{x},\mathbf{x}')+G^{\mathrm{H}}(\mathbf{x},\mathbf{x}')]\}\,\mathrm{d}S'. \tag{42}$$

8. Results

We begin by considering finite plates of circular and elliptical geometry. The circular finite plate acts as a check to validate numerical implementation since the vibration frequencies can be calculated straightforwardly, as specified in Leissa [1]. The following tables (Tables 1–4) of vibration frequencies ($\mu_l = k_l^2$) were computed and compared with some published values. These values were generated using 1000 panels around the boundary and truncating the sums in (11) from $-M$ to M, with $M = 10$–20 (depending on the degree of eccentricity of each ellipse and the relevant boundary condition). The values a and b

Table 1
Lowest four vibration frequencies for a circular plate of radius $a=1$ ($\star : \nu = 0.33, \dagger : \nu = 0.30$).

Results		Frequency values			
		1	2	3	4
Free − edge*	Lessia [1]	5.253	9.084	12.230	20.520
	Present	5.253	9.052	12.222	20.477
Clamped	Leissa [1]	10.216	21.260	34.880	51.040
	Present	10.205	21.235	34.832	50.960
Simply − supported†	Leissa and Narita [4]	4.953	13.898	25.613	39.957
	Present	4.948	13.933	25.676	40.056

Table 2
Lowest four vibration frequencies for a free elliptic plate ($\nu = 0.33$).

Results	b/a	Frequency values			
		1	2	3	4
Singh and Chakraverty [19]	0.8	6.091	6.563	12.184	14.665
Present		6.056	6.570	12.112	14.733
Singh and Chakraverty [19]	0.6	6.492	8.680	16.302	18.765
Present		6.472	8.641	16.242	18.714
Singh and Chakraverty [19]	0.4	6.662	12.827	17.037	25.946
Present		6.642	12.848	17.014	25.944

Table 3
Lowest four vibration frequencies for a simply-supported elliptic plate ($\nu = 0.3$).

Results	b/a	Frequency values			
		1	2	3	4
Singh and Chakraverty [21]	0.8	6.394	15.634	20.012	29.139
Present		6.391	15.636	20.022	29.137
Singh and Chakraverty [21]	0.6	9.763	19.566	33.122	33.777
Present		9.759	19.564	33.107	33.774
Singh and Chakraverty [21]	0.4	19.514	31.146	46.823	66.937
Present		19.494	31.192	46.787	66.921

Table 4
Lowest three vibration frequencies for a clamped elliptic plate.

Results	b/a	Frequency values		
		1	2	3
Singh and Chakraverty [20]	0.8	13.250	51.570	115.500
Present		13.281	51.738	115.376
Singh and Chakraverty [20]	0.6	20.340	79.170	177.400
Present		20.323	79.311	176.971
Singh and Chakraverty [20]	0.4	41.600	162.000	362.900
Present		41.801	161.461	364.890

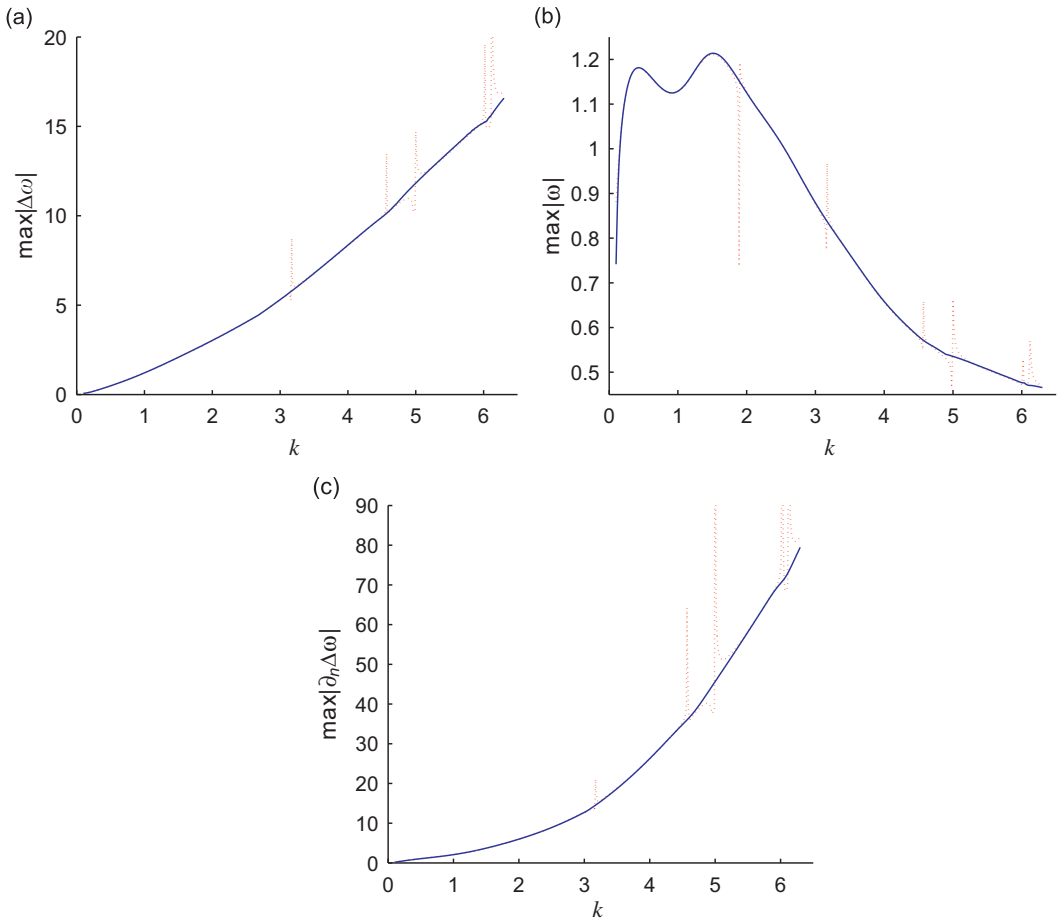

Fig. 3. Control of ill-conditioning effects for first unknown at cavity edge: (a) clamped edge conditions; (b) free-edge conditions; and (c) simply-supported conditions. The solid blue line represents the CBIEM solution and the broken red line represents the BIE solution without correction. (For interpretation of the references to colour in this figure legend, the reader is referred to the web version of this article.)

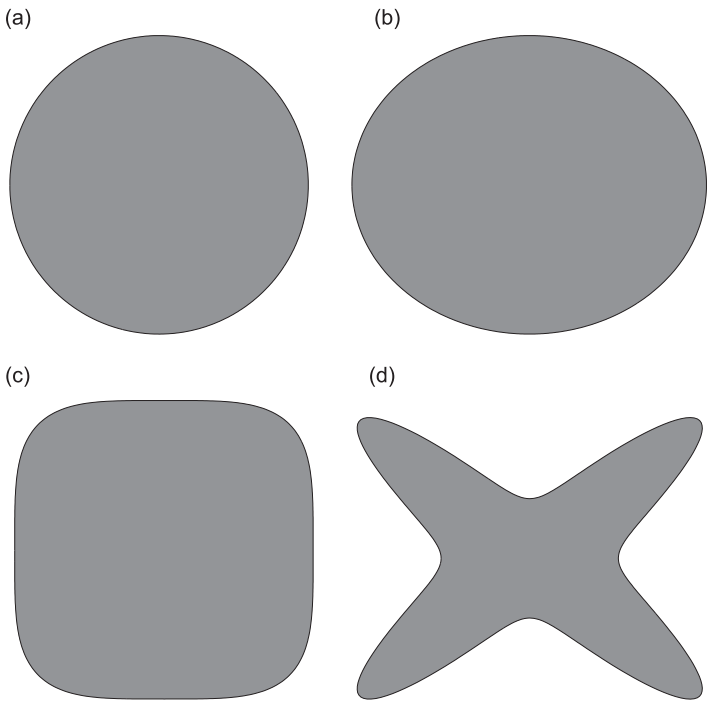

Fig. 4. Cavity geometries considered for computing plate displacement in Ω_∞: (a) circular cavity; (b) elliptical cavity; (c) L_4 cavity; and (d) star cavity.

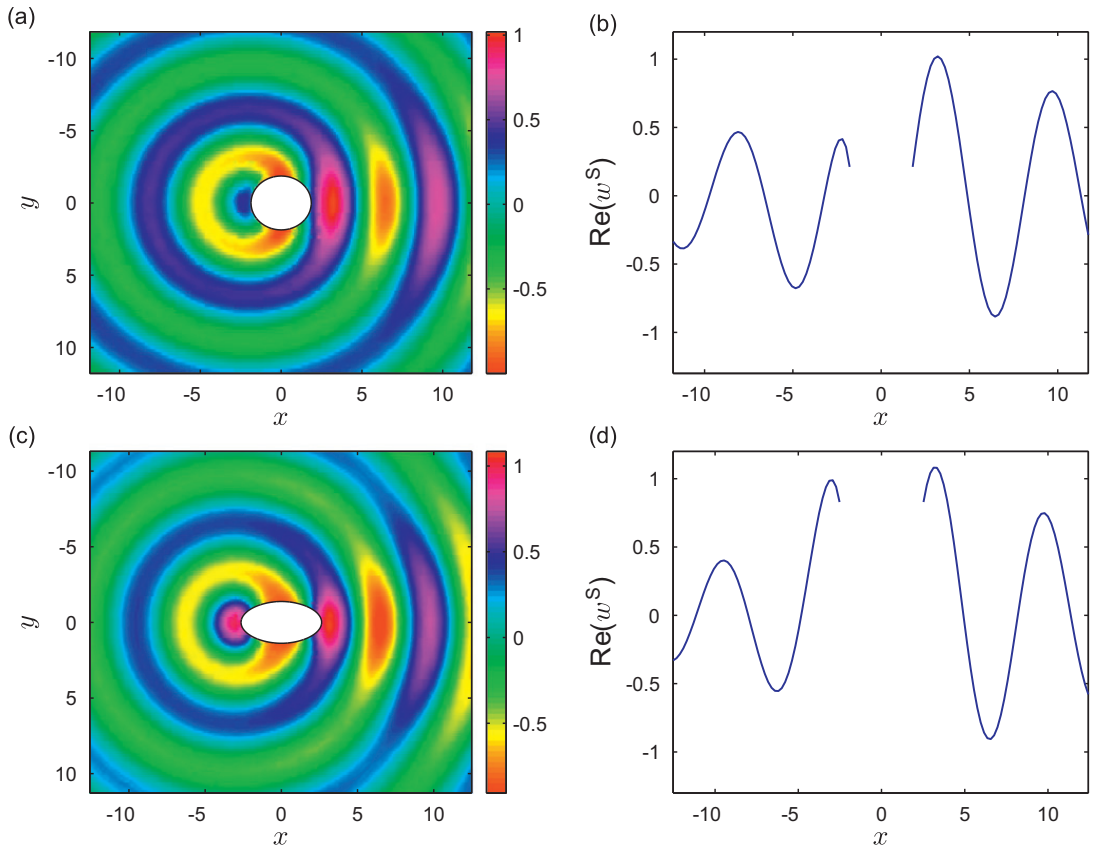

Fig. 5. (Color online) Scattered displacement field (real component) and line plot at $y=0$ under clamped boundary conditions for: (a,b) circular cavity and (c,d) elliptical cavity.

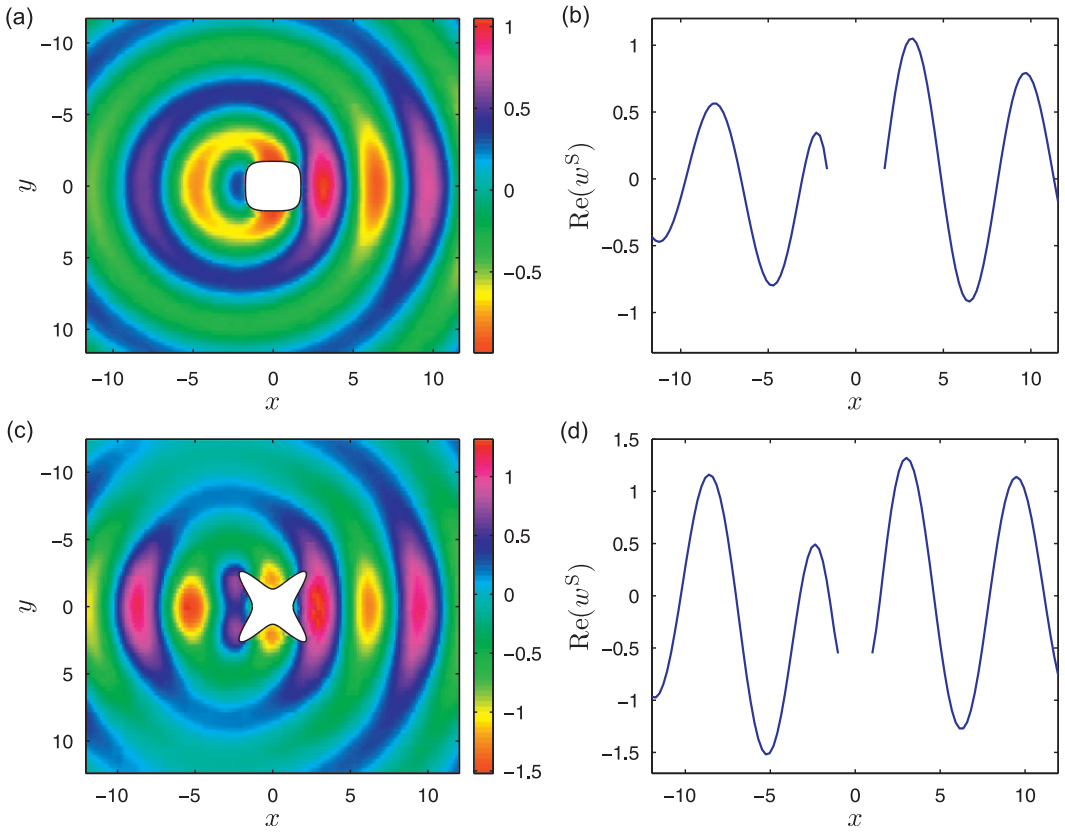

Fig. 6. (Color online) Scattered displacement field (real component) and line plot at $y=0$ under clamped boundary conditions for: (a,b) L_4 cavity and (c,d) star cavity.

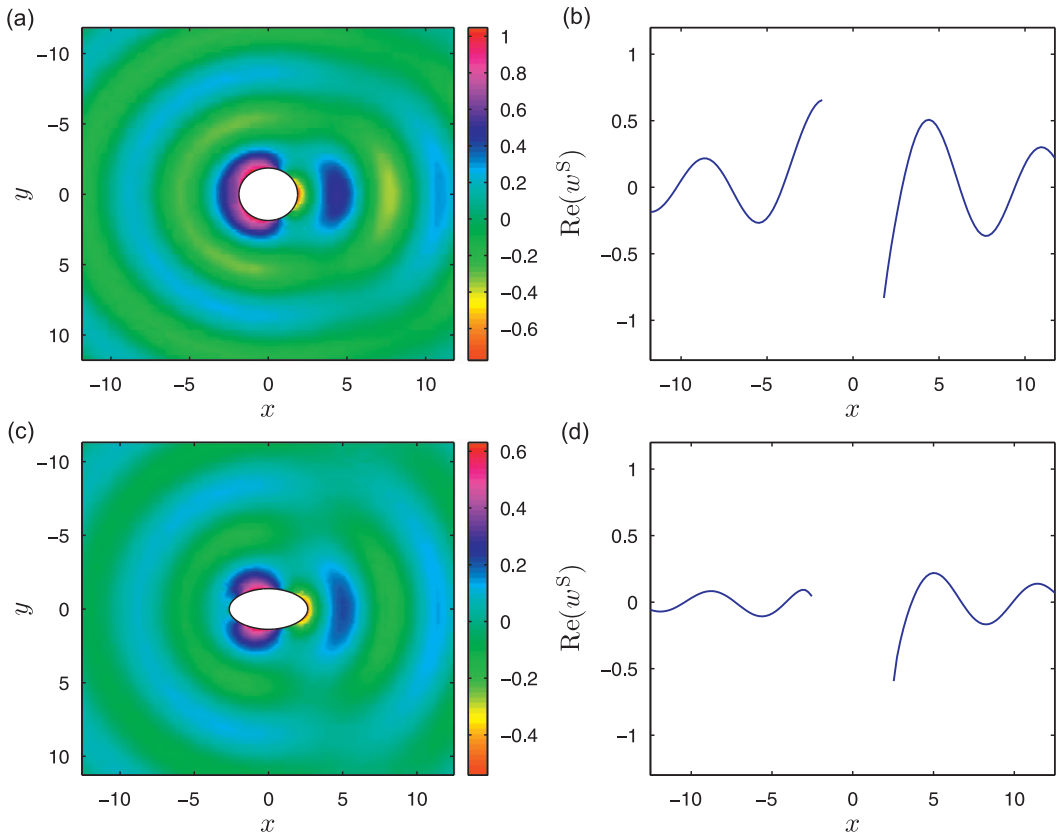

Fig. 7. (Color online) Scattered displacement field (real component) and line plot at $y=0$ under free-edge boundary conditions for: (a,b) circular cavity and (c,d) elliptical cavity.

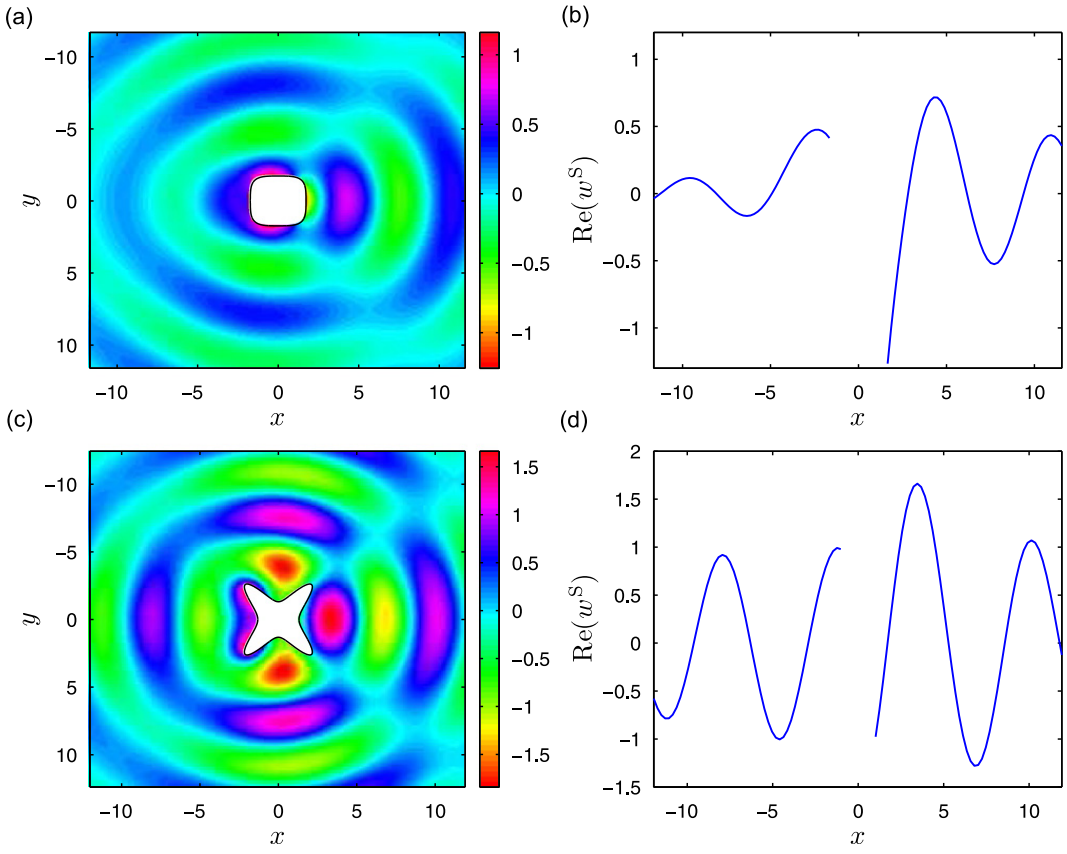

Fig. 8. (Color online) Scattered displacement field (real component) and line plot at $y=0$ under free-edge boundary conditions for: (a,b) L_4 cavity and (c,d) star cavity.

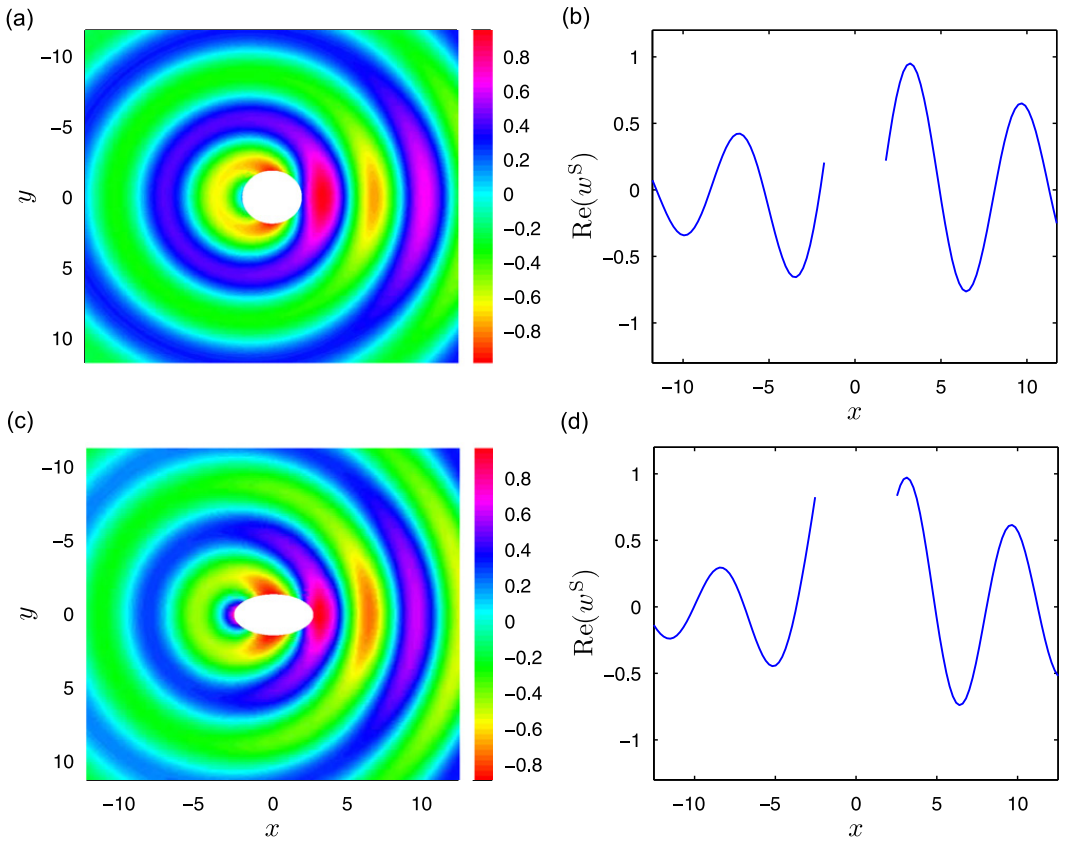

Fig. 9. (Color online) Scattered displacement field (real component) and line plot at $y=0$ under simply-supported boundary conditions for: (a,b) circular cavity and (c,d) elliptical cavity.

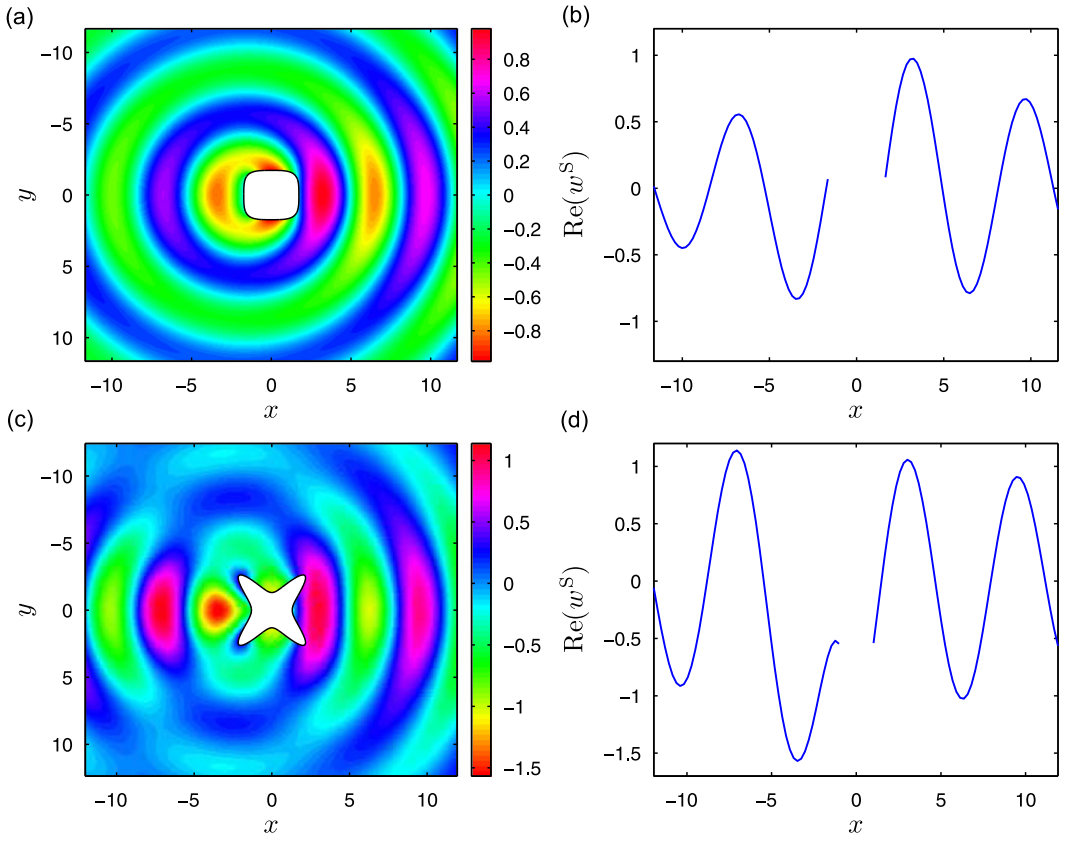

Fig. 10. (Color online) Scattered displacement field (real component) and line plot at $y=0$ under simply-supported boundary conditions for: (a,b) L_4 cavity and (c,d) star cavity.

denote the semi-major and semi-minor axes of an ellipse, with $a=1$ unless otherwise specified. We define v as the Poisson ratio.

The values from previous authors in the following tables are the lowest vibration frequencies corresponding to the first few modes of vibration (Singh and Chakraverty [19–21]). Accordingly for the case of a circular geometry we have chosen

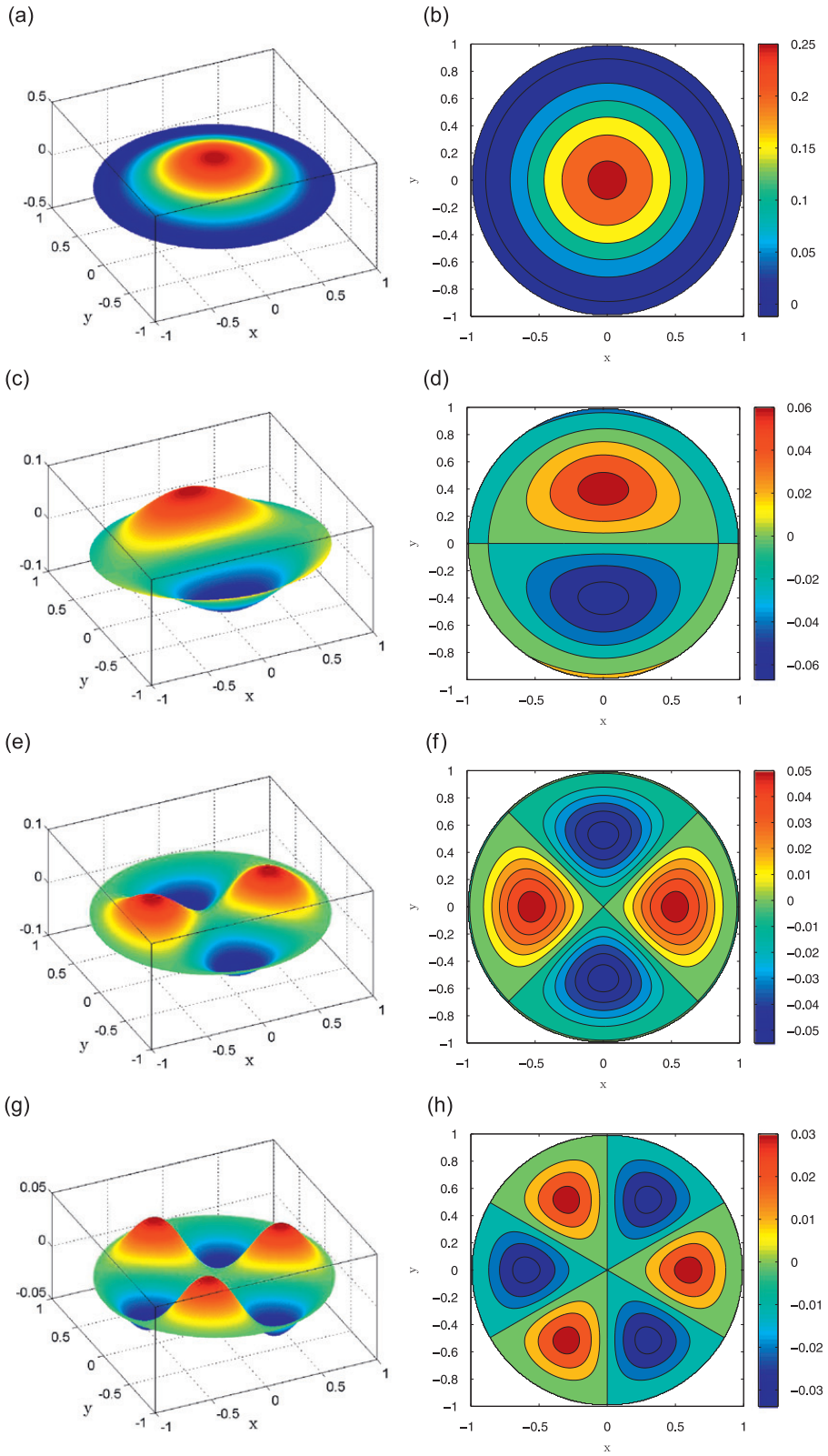

Fig. 11. (Color online) Plate displacement and associated contour plots for a clamped circular plate at: (a,b) $\mu=10.205$; (c,d) $\mu=21.235$; (e,f) $\mu=34.832$ and (g,h) $\mu=50.960$.

the values from Lessia [1] and Leissa and Narita [4] in a similar manner, although further frequency values are available in these publications.

Using the vibration frequency values from these tables, the following shapes for the displacement of the plate are generated in Figs. 11 and 12, for the case of a clamped circular plate and a free elliptic plate ($b/a=0.8$). These figures were generated using 400 panels at the plate boundary with $M=10$. The mode shapes generated in Fig. 11 for the circular plate

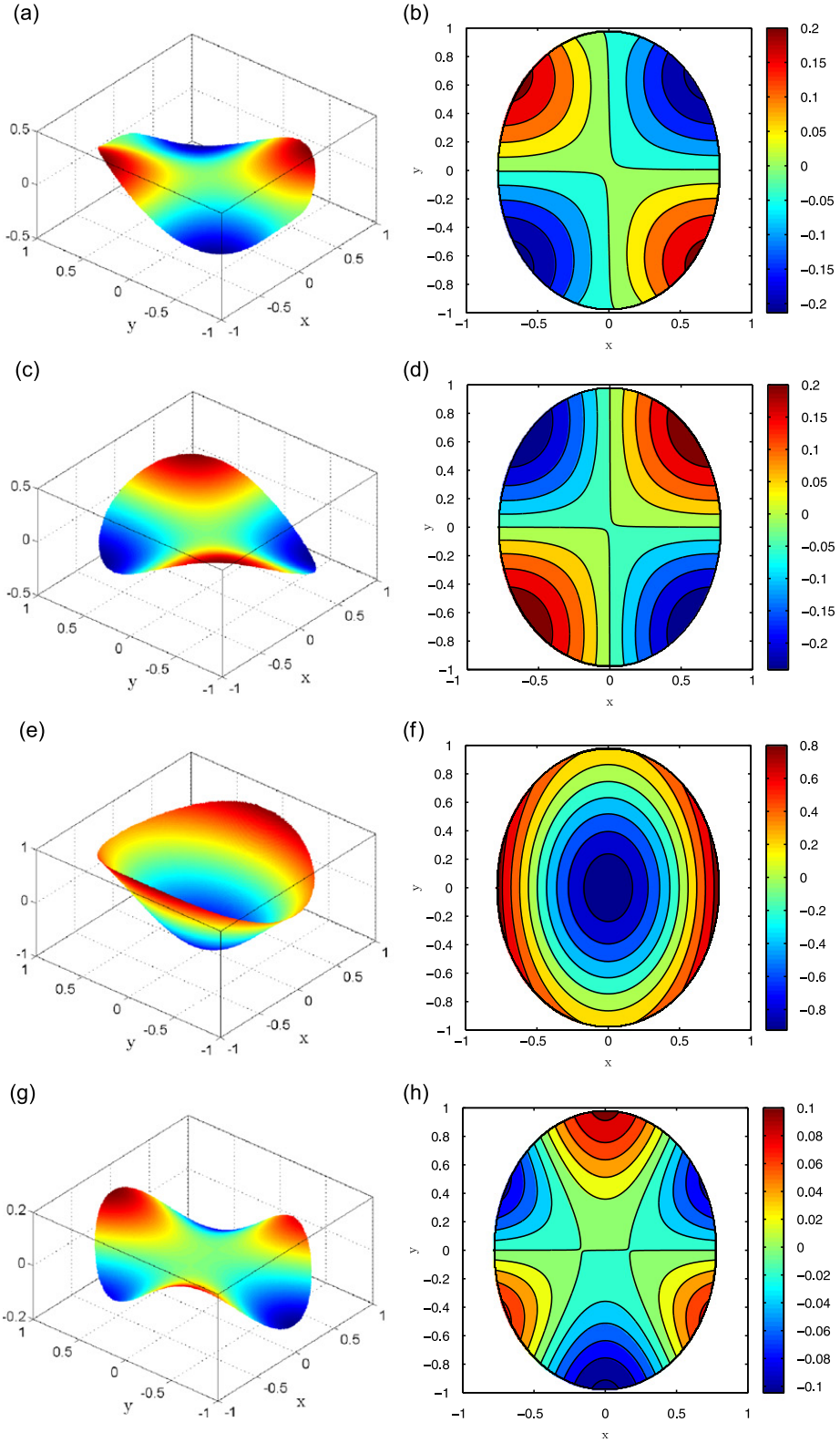

Fig. 12. (Color online) Plate displacement and associated contour plots for a free elliptic plate ($b/a=0.8$) at: (a,b) $\mu=6.056$; (c,d) $\mu=6.570$; (e,f) $\mu=12.112$ and (g,h) $\mu=14.733$.

are in keeping with the shapes that would be obtained by separation of variables, and the elliptical mode shapes in Fig. 12 are similar to the modes for a free-edge circular plate (but distorted) and also bear a strong resemblance to the shapes obtained in Singh and Chakraverty [20]. In Fig. 11(d), there is a small amount of error at the plate edge, which appears to arise from dipolar term effects.

We now consider the scattering problem by a finite closed cavity in an infinite plate. Firstly, to demonstrate the effectiveness of the combined boundary element method, the maximum absolute value of an unknown was plotted for varying k, using both the standard boundary integral equation approach and the combined boundary integral equation method.

From Fig. 3(a) to (c) , we can see that the CBIEM approach is able to efficiently control ill-conditioning when recovering unknowns at the cavity edge, for a range of frequency values, particularly at the irregular frequencies located at $k \approx 1.89, 3.17, 4.57, 5.00, 6.02$ and 6.12 (note that the first irregular frequency is less pronounced for the clamped and simply-supported cases). These figures were generated for an elliptical cavity ($b/a=2$, $a=1$) with $M=50$ solution modes, 500 panels, 30 CBIEM points and an incident potential $w^{\mathrm{I}} = J_0(kr)$.

The scattering displacement fields for circular, elliptical, L_4 and star cavities were generated for free-edge, clamped and simply-supported boundary conditions in Figs. 5–10, for an incident plane wave displacement incoming from the left. Corresponding line plots at $y=0$ are also shown. The cavities under consideration are shown in Fig. 4. Note that the L_4 cavity is called that due to its connection with the L_4 norm (for example, $x^4 + y^4 = 1$).

Primarily, the most interesting behaviour is exhibited by the star cavity which features back-scattering and resolution-blur for the clamped and simply-supported edge conditions in Figs. 6 and 10. In Fig. 8, we see channelling for the free-edge L_4 and star cavities, which originate from the corners of the cavities furthest to the right (in the direction of the incident wave propagation). It would appear that for all three boundary conditions, the scattering profile for the L_4 cavity qualitatively appears to be that of a stretched circular profile. There is no such relationship between the circular and elliptical cavities, with strong differences in the scattered displacement fields close to the point where the incident wave first strikes the cavity.

Our solution for the circular cavity shows strong agreement with the solution generated by the method outlined in Appendix A, for the three types of boundary conditions considered. The scattered displacement fields were generated using values $k=1$, $M=50$, 10 incident modes, 500 panels, 15 CBIEM points, and $\beta = 1/2$ where applicable, with the area of the cavities preserved at a constant value of 10. For example, the elliptical cavity has semi-major axes $a=1.2615$ and $b=2.5231$, so that the area $\pi ab \approx 10$ (and $b/a=2$).

9. Conclusions

In this paper we have demonstrated how to compute the displacement of an infinite plate, with a single arbitrarily shaped cavity about the origin, subject to an incident wave forcing in the frequency domain. Specifically, we have presented solutions for three types of boundary conditions, and have numerically demonstrated these with four geometries. It would be straightforward to implement more complicated geometries and other boundary conditions. We have also shown that by formulating this problem in terms of boundary integral equations, we encounter difficulties with irregular frequencies, which are controlled effectively using the combined boundary element method.

We have shown how to formulate the finite-plate vibration problem as a system of boundary integral equations, and have computed the first few eigenvalues for specified circular and elliptical plates. Additionally we have computed the modes of vibration for two geometries with two different boundary conditions. The results from these computations acts as validation of our numerical solution.

An algorithm to compute the eigenvalues is also discussed, based on a first-order expansion of the system, with results that generally agree well with literature values. In conclusion, the method we have described and verified will prove useful in a range of problems concerned with single cavities and inclusions. Of particular interest will be its application to arrays of cavities, which have already been shown by Movchan et al. [7] to have very interesting band-gap properties.

Acknowledgements

The authors would like to acknowledge the assistance of Dr. Garry Tee in his careful review of this article. We would also like to thank the reviewers for their helpful and constructive comments which have strengthened the paper.

Appendix A. Alternative approach for circular cavities

The displacement of the plate in Ω_∞ can be computed simply for the case of a circular cavity. This is outlined by Konenkov [5], Norris and Vemula [6], who expand the solution for a circle of radius a as follows:

$$w = w^{\mathrm{I}} + \sum_{n=-\infty}^{\infty} [A_n H_n^{(1)}(kr) + B_n H_n^{(1)}(\mathrm{i}kr)]\mathrm{e}^{\mathrm{i}n\theta}, \tag{A1}$$

where $H_n^{(1)}$ are Hankel functions of the first kind. A standard incident plane wave is then considered, and subsequently represented in terms of cylindrical waves via the Jacobi–Anger identity

$$w^{\mathrm{I}} = \mathrm{e}^{\mathrm{i}kr\cos\theta} = \sum_{n=-\infty}^{\infty} \mathrm{i}^n J_n(kr)\mathrm{e}^{\mathrm{i}n\theta}, \tag{A2}$$

Cakoni and Colton [24]. After applying the relevant boundary conditions at $r=a$, it is straightforward to obtain a system for the unknown coefficients in Eq. (A1). We demonstrate this for the case of free-edge boundary conditions, given by

$$\Delta w = \frac{\beta}{r}\left(\partial_r + \frac{1}{r}\partial_\theta^2\right)w, \tag{A3}$$

$$\partial_r \Delta w = -\frac{\beta}{r^2}\left(\frac{1}{r} - \partial_r\right)\partial_\theta^2 w. \tag{A4}$$

Applying these conditions at $r=a$ yields

$$\begin{bmatrix} a_n & b_n \\ c_n & d_n \end{bmatrix}\begin{bmatrix} A_n \\ B_n \end{bmatrix} = -\mathrm{i}^n \begin{bmatrix} e_n \\ f_n \end{bmatrix}, \tag{A5}$$

where

$$a_n = \left[\frac{\beta n^2}{a^2} - k^2\right]H_n^{(1)}(ka) - \frac{\beta k}{2a}[H_{n-1}^{(1)}(ka) - H_{n+1}^{(1)}(ka)], \tag{A6}$$

$$b_n = \left[\frac{\beta n^2}{a^2} + k^2\right]H_n^{(1)}(\mathrm{i}ka) - \frac{\mathrm{i}\beta k}{2a}[H_{n-1}^{(1)}(\mathrm{i}ka) - H_{n+1}^{(1)}(\mathrm{i}ka)], \tag{A7}$$

$$c_n = -\frac{k}{2}\left[\frac{\beta n^2}{a^2} + k^2\right][H_{n-1}^{(1)}(ka) - H_{n+1}^{(1)}(ka)] + \frac{\beta n^2}{a^3}H_n^{(1)}(ka), \tag{A8}$$

$$d_n = -\frac{\mathrm{i}k}{2}\left[\frac{\beta n^2}{a^2} - k^2\right][H_{n-1}^{(1)}(\mathrm{i}ka) - H_{n+1}^{(1)}(\mathrm{i}ka)] + \frac{\beta n^2}{a^3}H_n^{(1)}(\mathrm{i}ka), \tag{A9}$$

$$e_n = \left[\frac{\beta n^2}{a^2} - k^2\right]J_n(ka) - \frac{\beta k}{2a}[J_{n-1}(ka) - J_{n+1}(ka)], \tag{A10}$$

$$f_n = -\frac{k}{2}\left[\frac{\beta n^2}{a^2} + k^2\right][J_{n-1}(ka) - J_{n+1}(ka)] + \frac{\beta n^2}{a^3}J_n(ka). \tag{A11}$$

References

[1] A.W. Leissa, *Vibration of Plates*, NASA SP-160, U.S. Government Printing Office, Washington, D.C., 1969.
[2] K.F. Graff, *Wave Motion in Elastic Solids*, Dover Publications, New York, 1975.
[3] K. Itao, S.H. Crandall, Natural modes and natural frequencies of uniform, circular, free-edge plates, *Journal of Applied Mechanics* 46 (2) (1979) 448–454.
[4] A. Leissa, Y. Narita, Natural frequencies of simply supported circular plates, *Journal of Sound and Vibration* 70 (2) (1980) 221–229.
[5] Y. Konenkov, Diffraction of a flexural wave by a circular obstacle in a plate, *Journal of Soviet Physics: Acoustics* 10 (2) (1964) 153–156.
[6] A.N. Norris, C. Vemula, Scattering of flexural waves on thin plates, *Journal of Sound and Vibration* 181 (1995) 115–125.
[7] A.B. Movchan, N.V. Movchan, R.C. McPhedran, Bloch–Floquet bending waves in perforated thin plates, *Proceedings of the Royal Society A—Mathematical, Physical and Engineering Sciences* 463 (2007) 2505–2518.
[8] W.J. Parnell, P.A. Martin, Multiple scattering of flexural waves by configurations of inclusions in thin plates, *Wave Motion* 48 (2) (2011) 161–175.
[9] I.V. Andronov, B.P. Belinskii, Scattering of a flexural wave by a finite straight crack in an elastic plate, *Journal of Sound and Vibration* 180 (1) (1995) 1–16.
[10] R. Porter, D.V. Evans, Diffraction of flexural waves by finite straight cracks in an elastic sheet over water, *Journal of Fluids and Structures* 23 (2) (2007) 309–327.
[11] L.G. Bennetts, T.D. Williams, Wave scattering by ice floes and polynyas of arbitrary shape, *Journal of Fluid Mechanics* 662 (2010) 5–35.
[12] R.E. Kleinman, G.F. Roach, Boundary integral equations for the three-dimensional Helmholtz equation, *Society for Industrial and Applied Mathematics Review* 16 (2) (1974) 214–236.
[13] R.E. Kleinman, G.F. Roach, On modified Green's functions in exterior problems for the Helmholtz equation, *Proceedings of the Royal Society of London* 383 (1982) 313–332.
[14] C.M. Linton, P. McIver, *Handbook of Mathematical Techniques for Wave/Structure Interactions*, Chapman & Hall, New York, 2001.
[15] S.M. Lau, G.E. Hearn, Suppression of irregular frequency effects in fluid–structure interaction problems using a combined boundary integral equation method, *International Journal for Numerical Methods in Fluids* 9 (1989) 763–782.
[16] P.A. Martin, On the null-field equations for the exterior problems of acoustics, *Quarterly Journal of Mechanics and Applied Mathematics* 33 (1980) 385–395.
[17] J.G. Yardley, R.C. McPhedran, N.A. Nicorovici, L.C. Botten, Addition formulas and the Rayleigh identity for arrays of elliptical cylinders, *Physical Review E* 60 (5) (1999) 6068–6080.

[18] M. Stern, A general boundary integral formulation for the numerical solution of plate bending problems, *International Journal of Solids and Structures* 15 (10) (1979) 769–782.
[19] B. Singh, S. Chakraverty, Transverse vibration of completely-free elliptic and circular plates using orthogonal polynomials in the Rayleigh–Ritz method, *International Journal of Mechanical Sciences* 33 (9) (1991) 741–751.
[20] B. Singh, S. Chakraverty, Transverse vibration of circular and elliptic plates with quadratically varying thickness, *Applied Mathematical Modelling* 16 (1992) 269–274.
[21] B. Singh, S. Chakraverty, Transverse vibration of simply supported elliptic and circular plates using boundary characteristic orthogonal polynomials in two variables, *Journal of Sound and Vibration* 152 (1) (1992) 149–155.
[22] M. Kitahara, *Boundary Integral Equation Methods in Eigenvalue Problems of Elastodynamics and Thin Plates*, Elsevier, Amsterdam, 1985.
[23] A.J. Burton, G.F. Miller, The application of integral equation methods to the numerical solution of some exterior boundary-value problems, *Proceedings of the Royal Society of London* 323 (1971) 201–210.
[24] F. Cakoni, D. Colton, *Qualitative Methods in Inverse Scattering Theory*, Springer, Heidelberg, 2006.